Ab initio cluster-model study of the electronic ground-state and photoemission properties of NiN_2 and NiCO: Models for chemisorption

C. M. Kao
Department of Physics, University of Pennsylvania, Philadelphia, Pennsylvania 19104

R. P. Messmer
General Electric Corporate Research and Development Center, Schenectady, New York 12301
and Department of Physics, University of Pennsylvania, Philadelphia, Pennsylvania 19104
(Received 8 June 1984; revised manuscript received 14 January 1985)

The ground state of the linear NiN_2 cluster is found, from generalized valence-bond configuration-interaction calculations, to be a $^1\Sigma^+$ state with a short Ni—N distance of 1.64 Å and a Ni—N_2 dissociation energy of 0.8 eV. In this $^1\Sigma^+$ state near the calculated equilibrium internuclear distance, the electronic wave function may be characterized as arising from a significant admixture of the Ni $3d^{10}$ configuration, and the bonding of the N_2 molecule to the Ni atom may be characterized as N_2 σ donation and Ni $3d\pi$ backward donation. Low-lying excited states ($^3\Sigma^+$, $^3\Delta$, and $^3\Pi$) arising from the Ni $3d^9 4s^1$ configuration are also studied. Mulliken population analyses, dipole moments, and vibrational and photoemission properties are calculated. Parallel calculations are also performed for the linear NiCO molecule. The $^1\Sigma^+$ states of both NiN_2 and NiCO are good models for the chemisorption of N_2 and CO on a Ni surface, with regard to the downward shift of the molecular stretching frequency in the interacting systems, the photoemission satellite structure, and the orientation of the dipole moments (with a net electron transfer from Ni to N_2 or CO).

I. INTRODUCTION

In the present study we consider the linear NiN_2 system in order to assess the effects of electronic correlation in the Ni—N_2 interaction, on the assumption that a better understanding of the nature of bonding in linear NiN_2 also may shed some light on the chemisorption problem. The choice of the linear geometry has its experimental basis in the vibrational properties of NiN_2 isolated in matrices[1] as well as the angle-resolved photoemission data and vibrational intensities for N_2 chemisorbed on Ni surfaces.[2] The complexity of treating the electronic correlation problem for transition-metal-molecule interactions is such that it necessitates the consideration of such rather limited clusters at present. However, for situations where only the d^9s^1 configuration of Ni is important, as may be the case in treating precursor states to chemisorption on Ni surfaces, larger clusters may be treated. Such considerations are discussed elsewhere.[3]

The electronic structure of linear NiN_2 previously has been studied theoretically by Bagus and co-workers.[4] They found the ground state to be a $^3\Delta$ state with a rather long Ni—N bond distance (>2.2 Å) and a small Ni—N_2 bond energy (<0.1 eV) on the basis of Hartree-Fock (HF) calculations. In contrast, the chemisorption energy of N_2 on Ni surfaces,[5] as well as the Ni—N_2 bond dissociation energy in $Ni(CO)_3N_2$,[6] is ~ 0.5 eV. Furthermore, the N—N and Ni—N_2 stretching frequencies of NiN_2 (2090 and 466 cm^{-1} in an Ar matrix)[1] and of N_2 chemisorbed on the Ni(110) surface (2186 and 323 cm^{-1}) (Ref. 2) indicate appreciable Ni—N_2 interaction. Note that the vibrational frequency of the isolated N_2 molecule[7] is 2359 cm^{-1}. Thus, one might question the conclusion of these previous calculations that the ground state of NiN_2 is a $^3\Delta$ state.

In the more familiar linear NiCO case, a $^1\Sigma^+$ state (with the Ni $3d^{10}$ configuration being dominant) has been predicted as the ground state from *ab initio* configuration interaction[8] (CI) and $X\alpha$ calculations.[9] We have also come to the same conclusion and will present our calculations on NiCO in this paper. The Ni—CO bond is usually described in terms of (CO) σ donation and (Ni) π backward donation. These interactions are facilitated in the Ni $3d^{10}$ configuration, because the CO 5σ is no longer antibonding to the Ni $4s$ electron but is bonding to Ni (as the Ni $4s$ orbital is nominally unoccupied in the $3d^{10}$ configuration), which results in a shorter Ni—CO distance and allows better Ni π backward donation. On the other hand, it requires 1.74 eV for the excitation from Ni $3d^9 4s^1$ (^3D) to $3d^{10}$ (^1S). Thus, the relevant question in the present context is whether the bonding interaction in NiN_2 is sufficiently strong to offset this excitation energy and result in the $^1\Sigma^+$ state being the ground state.

Indeed, we have found that the ground state of NiN_2 is the $^1\Sigma^+$ state. We have reached this conclusion from CI calculations based on generalized-valence-bond (GVB)[10] wave functions (i.e., GVB-CI). Besides studying the $^1\Sigma^+$ state which in the dissociation limit corresponds to N_2+Ni (^1D, d^9s^1), we also have considered three triplet states, the $^3\Sigma^+$, $^3\Delta$, and $^3\Pi$, which correspond to ^3D Ni (d^9s^1) with Ni d holes in $d\sigma$, $d\pi$, and $d\delta$ orbitals, respectively. Although the Ni $3d^9 4s^1$ (^1D) configuration occurs at the dissociation limit of the NiN_2 (and NiCO) $^1\Sigma^+$ state, the Ni d^{10} configuration is quite important near the

equilibrium geometry of this state, according to our analysis of the wave functions. Details of the calculations are presented in Sec. II, followed by results and a discussion of the electronic structure of NiN_2 in Sec. III in which the nature of the bonding will be addressed in some depth in terms of energetics, charge distribution, vibrational and photoemission properties, and contrasted with corresponding results for NiCO. In Sec. IV our understanding of the bonding in NiN_2 will be used to discuss the chemisorption of N_2 on Ni surfaces. A brief summary is presented in Sec. V.

II. CALCULATIONAL METHODS

All of the calculations reported here are variational in nature and the wave functions have the generic form

$$\Psi=\sum_i c_i\Phi_i \ , \tag{1}$$

where the Φ_i's are Slater determinants made up of orthogonal one-electron orbitals. For example, if $\Psi\cong\Phi_1=\mathscr{A}[\phi_1\phi_1\cdots\phi_n\phi_n\alpha\beta\cdots\alpha\beta]$ with $\langle\phi_i\,|\,\phi_j\rangle=\delta_{ij}$, one obtains the well-known Hartree-Fock approximation and the optimal forms of the ϕ_i's are determined variationally. An approximation which introduces intrapair correlation for pairs of electrons is the perfect-pairing (PP) form of the generalized valence-bond method,[10] the wave function is

$$\Psi\cong\Phi_{PP}=\mathscr{A}[(\lambda_{1b}\phi_{1b}\phi_{1b}-\lambda_{1a}\phi_{1a}\phi_{1a})\cdots \times(\lambda_{nb}\phi_{nb}\phi_{nb}-\lambda_{na}\phi_{na}\phi_{na})\alpha\beta\cdots\alpha\beta] \ . \tag{2}$$

This is of the form of Eq. (1) which can be seen easily by expanding Eq. (2). In this method both the λ_i's and the ϕ_i's (referred to as natural orbitals) are determined variationally. However, Eq. (2) can be transformed into the following form:

$$\begin{aligned}\Phi_{PP}&=\mathscr{A}[(\psi_{1\mu}\psi_{1\nu}+\psi_{1\nu}\psi_{1\mu})\cdots \times(\psi_{n\mu}\psi_{n\nu}+\psi_{n\nu}\psi_{n\mu})\alpha\beta\cdots\alpha\beta] \\ &=\mathscr{A}[(\psi_{1\mu}\psi_{1\nu}\cdots\psi_{n\mu}\psi_{n\nu})(\alpha\beta-\beta\alpha)\cdots(\alpha\beta-\beta\alpha)] \ ,\end{aligned} \tag{3}$$

where it is apparent that there is one spatial orbital per electron and hence an orbital interpretation of the wave function is possible in spite of the fact that Eq. (2) is made up of 2^n Slater determinants. The ψ_i's are referred to as perfect-pairing orbitals, and satisfy the relations $\langle\psi_{i\mu}\,|\,\psi_{j\nu}\rangle=S_i^{\mu\nu}\delta_{ij}$, which are known as the strong-orthogonality constraints.

The determinants contained in Eq. (2) are all of the form where either ϕ_{ib} or ϕ_{ia} is doubly occupied but they are never simultaneously occupied. However, one can construct various projection operators, O_{CI}, which operate on Φ_{PP} and generate such additional terms in the expansion of Eq. (1). Such additional determinants among others are the basis of the GVB-CI method,[10] which relaxes the strong-orthogonality constraints and allows for interpair correlation effects.

The basis sets for the first-row atoms (C, N, and O) used in our calculations were of valence double zeta plus polarization quality.[11] For Ni, the Ar core was replaced by a modified effective potential,[12] the $3d$, $4s$, and $4p$ basis sets were of double-zeta quality.[13] The s combinations of d-type basis functions were excluded.

In all calculations the GVB perfect-pairing wave functions[10] were first obtained. The three bonds in the N_2 and CO molecules (one σ and two π bonds) and the 10 valence electrons (outside the Ar core) in the Ni atom moiety were pair-wise correlated. Thus, for the NiN_2 there were eight GVB pairs in the $^1\Sigma^+$ state and seven pairs plus two open-shell orbitals in the $^3\Sigma^+$, $^3\Delta$, and $^3\Pi$ states. The orbitals were required to have C_{2v} symmetry.

Additional interpair correlation effects and the relaxation of the strong-orthogonality constraint were achieved by CI calculations employing all occupied valence natural orbitals (a total of 18). The configurations in the CI calculations were chosen such that the wave functions corresponded to double-excitation CI (DCI) on N_2 (or on CO) times DCI on Ni at the dissociation limit ($Ni+N_2$ or $Ni+CO$), with the restriction that excitations into and out of the Ni δ-type $3d$ orbitals ($3d_{xy}$ and $3d_{x^2-y^2}$) were excluded and that a maximum number of six open shells was allowed. We shall designate such CI calculations as GVB-D*DCI. They were designed to describe both the $^1\Sigma^+$ and the triplet states in a balanced fashion *(vide infra)*. For the $^3\Pi$ state, the $d_{x^2-y^2}$ and the σ-type d_{z^2} orbitals become mixed when C_{2v} symmetry is used; in order to keep the number of configurations reasonable, this mixing was not allowed by forcing the $d_{x^2-y^2}$-type basis functions to be pure δ type (a_2 in C_{2v}). This procedure increased the $^3\Pi$ energy by less than 0.001 hartree at the PP level. Thus the resulting numbers of configurations were 3204, 2592, 4145, and 2985 for the $^1\Sigma^+$, $^3\Sigma^+$, $^3\Delta$, and $^3\Pi$ states, respectively.[14] We also did a few CI calculations, designated as GVB-D*QCI, which corresponded to DCI on N_2 (or on CO) times quadruple-excitation CI (QCI) on Ni, with the restriction that excitations among orbitals of different symmetry (C_{2v}) types were excluded. These GVB-D*QCI calculations are not dissociation consistent and were used mainly to indicate the importance of the Ni $3d^{10}$ configuration in the $^1\Sigma^+$ states *(vide infra)*.

Because the orbitals were optimized at the GVB-PP level and no virtual orbitals were used in the CI calculations, the $^1\Sigma^+$ wave functions obtained are not optimal, i.e., the GVB-PP wave functions, which do not contain interpair correlation, result in a $^1\Sigma^+$ state better characterized as Ni d^9s^1, rather than as d^{10}. It was realized that a reasonable procedure for obtaining the $^1\Sigma^+$ state of NiN_2, is to start with such a converged GVB-PP wave function and then freeze the doubly occupied Ni $3d_{z^2}$ orbital and allow the other orbitals to reoptimize. Subsequently these latter orbitals are frozen and the $3d_{z^2}$ correlated pair is optimized. Although this new set of orbitals yields a much worse energy at the PP level, it provides a much better energy at the CI level. This procedure for obtaining the Ni d^{10} configuration was used in the calculations for the NiN_2 $^1\Sigma^+$ state, but was not applied to the $^1\Sigma^+$ state of NiCO. Our CI results very probably underestimate the Ni—CO and Ni—N_2 interactions, especially for the $^1\Sigma^+$ states, because

TABLE I. Calculated excitation energies (eV) of the Ni atom.

Final state	HF	GVB-PP	GVB-DCI	GVB-QCI	Expt.[a]
^1D (d^9s^1)	0.471	0.467	0.351		0.332
^1S (d^{10})	4.21	3.62	2.19	2.01	1.74
$3d^94p^1$	4.22	4.24	4.31		3.51[b]
^2D (d^9)	7.97	7.97	8.07		7.66
Reference (initial state)[c]					
^3D (d^9s^1)	−40.540 50	−40.558 92	−40.608 71	−40.611 84	

[a]Reference 15. Values quoted in the table are obtained by weight averaging the spin-orbit fine-structure splittings.
[b]The experimental value quoted corresponds to $^3P^0 \leftarrow {}^3D$. There are three triplet terms ($^3P^0$, $^3F^0$, and $^3D^0$) associated with $3d^94p^1$, with a spread of 0.12 eV. Calculated values are for a triplet configuration which is an average of the states with $L = 1,2,3$.
[c]Calculated total energy of the ^3D state in hartree units.

we did not use excitations into virtual orbitals to allow for changes in the orbital shapes.

III. RESULTS AND DISCUSSION

A. Electronic structure and bonding

As we are interested in states of NiN_2 and NiCO that have quite different Ni character, i.e., a mixture of $3d^{10}$ and $3d^94s^1$ for $^1\Sigma^+$, and nearly pure $3d^94s^1$ for $^3\Sigma^+$, $^3\Delta$, and $^3\Pi$, it is important to be able to describe the Ni atomic spectrum reasonably well, especially for the d^{10}-d^9s^1 separation, at the same level of calculation to be employed for NiN_2 and NiCO. In Table I, we compare a few calculated quantities with experiment:[15] the ^1D (d^9s^1)$\leftarrow {}^3D$ (d^9s^1), ^1S (d^{10})$\leftarrow {}^3D$, and $3d^94p^1$ (triplets) $\leftarrow {}^3D$ excitation energies, and the ionization potential for the Ni atom. This table serves mainly to indicate the importance of correlation effects for the $d^{10}\leftarrow d^9s^1$ excitation and the quality of the basis set used. It is clear that a reasonable description of the separation between the $^1\Sigma^+$ and triplet states of NiN_2 and NiCO will require CI calculations involving at least double excitations on the Ni atom, should the Ni d^{10} configuration be an important component in the $^1\Sigma^+$ states.

Results of calculations for the isolated N_2 and CO are summarized in Tables II and III, respectively. The equilibrium geometries and the vibrational frequencies, as well as the dipole moment of CO, agree quite well with the experimental values. In Figs. 1 and 2, contour plots of the occupied valence orbitals are shown for N_2 and CO, respectively. Note that the carbon lone pair of CO is more diffuse than the nitrogen lone pairs in N_2 and that the π orbitals in CO are polarized towards oxygen (which is related to the usual description in the molecular orbital approximation that the virtual 2π orbital is localized on the carbon atom).

Having considered the isolated components, we can now investigate the interaction between Ni and the molecules in the NiN_2 and NiCO systems. We will look at the wave functions first, in terms of orbital plots, dipole moments, and Mulliken population analysis.[16] This is followed by a discussion of the energetics and a study of the vibrational and photoemission spectroscopies of these systems.

The orbitals for the $^1\Sigma^+$ and the $^3\Sigma^+$ states of NiN_2 at the calculated equilibrium geometries are shown in Figs. 3, 4, and 5, 6, respectively. The orbitals for the $^3\Delta$ state are similar to those for the $^3\Sigma^+$ state, and therefore are not shown (but of course the $^3\Sigma^+$ state has a $d\sigma$ hole while the $^3\Delta$ state has a $d\delta$ hole). Likewise, the orbitals for the corresponding states of NiCO have more or less the same characteristics and are not shown. It is quite clear from the contrast between Figs. 4 and 6 that there is significant π backward donation from Ni in the $^1\Sigma^+$ state and polarization of the Ni $4s$ orbital away from N_2 in the $^3\Sigma^+$ state.

Potential curves and dipole moments for the states of NiN_2 and NiCO have been evaluated at the points listed in Tables IV and V, respectively. Note the drastic changes in the dipole moments in going from the GVB-PP to the GVB-D*DCI description for the $^1\Sigma^+$ states. The signs of the dipole moments at the equilibrium geometries for the $^1\Sigma^+$ states are opposite to those of the triplet states. In the $^1\Sigma^+$ states, the negative end of the dipole points toward the N_2 or CO, which suggests an electronic charge shift from Ni to N_2 and, to a larger extent, from Ni to CO.

In terms of the Mulliken population analysis (we omit

TABLE II. Calculations on the N_2 molecule. GVB-DCI calculations.

	R (Å)	$E+109.0$ (hartree)	ν (cm^{-1})	k (mdyn/Å)
	1.0715	−0.087 88		
	1.1215	−0.093 34		
	1.1715	−0.085 46		
Calc.[a]	1.1170	−0.093 46	2374	22.4
Expt.[b]	1.0977		2359	

[a]Obtained from quantities in the first three rows above. The GVB-PP energy at this geometry is −109.032 99 hartree.
[b]Reference 7.

TABLE III. Calculations on the CO molecule. GVB-DCI calculations.

	R (Å)	$E+112.0$ (hartree)	ν (cm^{-1})	k (mdyn/Å)	μ (D)[a]
	1.0975	−0.873 09			
	1.1475	−0.878 22			
	1.1975	−0.872 11			
Calc.[b]	1.1453	−0.878 26	2203	18.9	0.238
Expt.[c]	1.1283		2170		0.122

[a]Positive if the negative end of the dipole points towards the carbon atom.
[b]Obtained from quantities in the first three rows above. The GVB-PP energy at this geometry is −112.817 69 hartree.
[c]Reference 7 and J. S. Meutner, J. Mol. Spectrosc. **55**, 490 (1975) (dipole moment).

consideration of the $^3\Pi$ states as they are the least bound, cf. Tables IV and V) presented in Tables VI and VII for the states of NiN_2 and NiCO, respectively, we make the following general observations.

(a) In all states of both NiN_2 and NiCO, the σ-type populations on the molecules (N_2 and CO) are shifted towards the Ni atom. Within the molecule, the decrease in the σ population is greater for the atom closest to the Ni atom (C or N_a). Among the electronic states at their respective equilibrium geometries, the decrease is greatest in the $^1\Sigma^+$ states. However, at the same Ni-C or Ni-N_a distance, the decrease at atom C or N_a is largest in the $^3\Sigma^+$ state and smallest in the $^3\Delta$ state, while the decrease at the other atom (O or N_b) is largest in the $^1\Sigma^+$ state. Basically, the above observation is consistent with the σ-donation mechanism. As these σ-type populations are

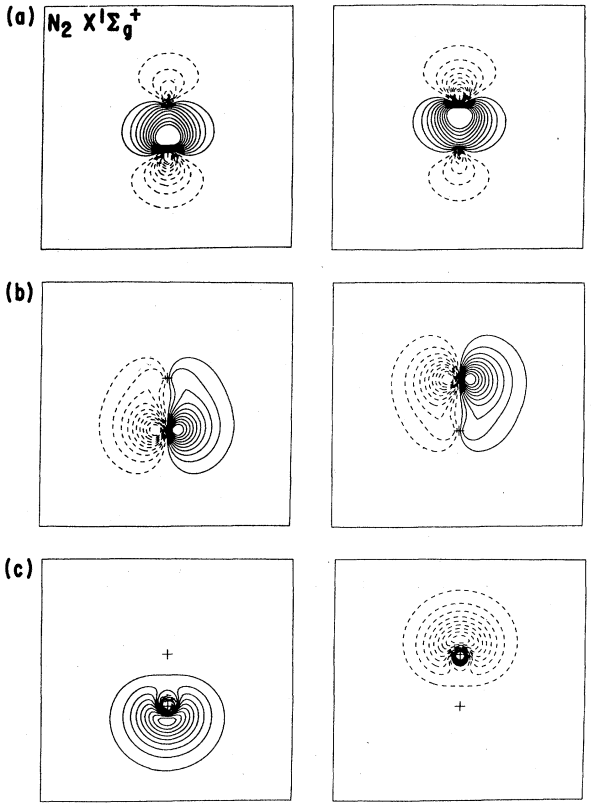

FIG. 1. Valence orbital contour plots (in the **y-z** plane) of the GVB-PP(3P) wave function for N_2. (a) GVB σ-bond pair; (b) GVB π_y-bond pair, there is another equivalent pair (not shown) in the **x-z** plane; (c) the two doubly occupied lone pairs obtained from combinations of the canonical orbitals.

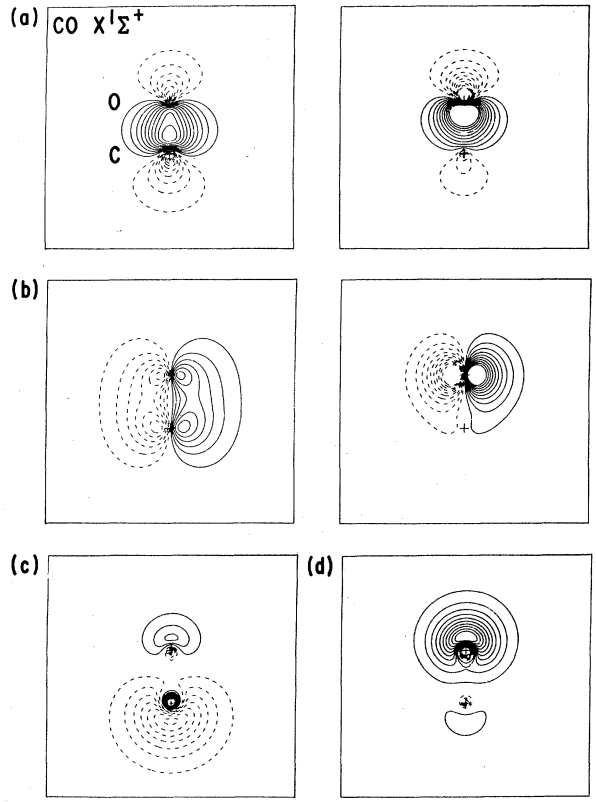

FIG. 2. Valence orbital contour plots (in the **y-z** plane) of the GVB-PP(3P) wave function for CO. (a) GVB σ-bond pair; (b) GVB π_y-bond pair, there is another equivalent pair (not shown) in the **x-z** plane; (c) carbon lone pair (doubly occupied); (d) oxygen lone pair (doubly occupied).

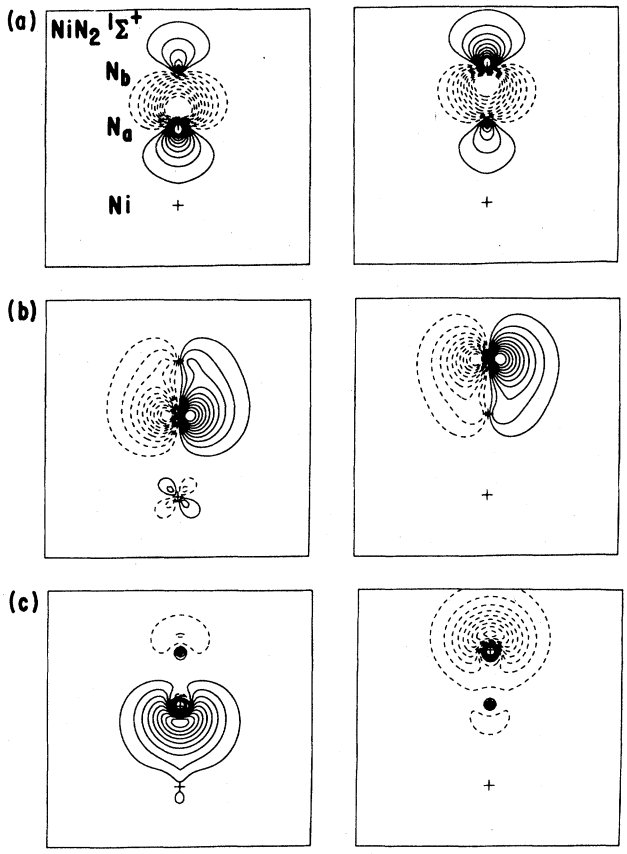

FIG. 3. N_2-derived valence orbital contour plots (in the **y-z** plane) of the GVB-PP wave function for the NiN_2 $^1\Sigma^+$ state at the calculated equilibrium geometry. (a) N_2 GVB σ-bond pair; (b) N_2 GVB π_y-bond pair, there is another equivalent pair (not shown) in the **x-z** plane; (c) the two doubly occupied N_2 lone pairs obtained from combinations of the canonical orbitals.

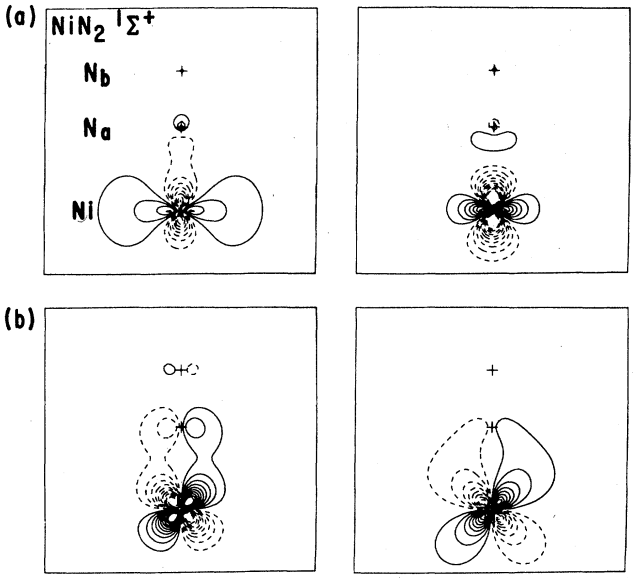

FIG. 4. Ni-derived valence orbital contour plots (in the **y-z** plane) of the GVB-PP wave function for the NiN_2 $^1\Sigma^+$ state at the calculated equilibrium geometry. (a) Ni $3d\sigma+4sp\sigma$ pair; (b) Ni $3d\pi_y$ pair, there is another equivalent pair (not shown) in the **x-z** plane.

also interdependent with π-type populations, it is not appropriate to consider all details independently. But the differences between $^3\Sigma^+$ and $^3\Delta$ states are obviously due to better σ donation in the $^3\Sigma^+$ states because of the localized Ni $3d\sigma$ hole.

(b) The changes in the π-type populations in the CO and N_2 molecules are such that at C and N_a there are increases in all states, but at O and N_b there are increases in the $^1\Sigma^+$ states and decreases in the triplet states. Again, the polarizations of these π-type electrons are interdependent with σ-type populations and π backward donation, as a result of the screening mechanism (to minimize charge build up).

(c) The Ni $3d\sigma+3d\delta$ population is slightly greater than 5 in the $^3\Sigma^+$ states, somewhat less than 5 in the $^3\Delta$ states, and is closer to 6 than to 5 in the $^1\Sigma^+$ states. Note that this population is 6 for a pure Ni $3d^{10}$ configuration and 5 for a pure $3d^9 4s^1$ configuration with a $3d\sigma$ hole.

(d) The Ni $4s$ population is close to 1 in the $^3\Delta$ and $^3\Sigma^+$ states (slightly larger in the $^3\Delta$ states), and much less than 1 in the $^1\Sigma^+$ states. This observation, together with (c), supports our characterization of the $^1\Sigma^+$ states as significantly involving a Ni $3d^{10}$ configuration.

(e) Although the Ni π population decreases in all states, the effect is largest for the $^1\Sigma^+$ states. This decrease, or π backward donation, may be correlated with the Ni $3d$ ionization energies for different configurations. Experimentally,[15] the $d^9 \leftarrow d^{10}$ ionization energy is 5.8 eV, while the $d^8 s^1$ (^4F)$\leftarrow d^9 s^1$ (^3D) ionization energy is 8.7 eV. Based on this energetic information, one may understand how the $^1\Sigma^+$ states (with significant Ni d^{10} like character) involve more π backward donation. Along this line, the π backward donation in the corresponding Pd and Pt complexes is expected to be less significant, because of the higher $d^9 \leftarrow d^{10}$ ionization energies (8.5 and 9.3 eV for Pd and Pt, respectively). Indeed, the downward shifts of the N_2 or CO stretching frequencies, which reflect the degree of π backward donation *(vide infra)*, are smaller in Pd and Pt complexes.[1,17]

(f) The Ni $4p_z$ (z is the molecular axis) population is largest in the $^3\Delta$ states. This population is a measure of the Ni $4s$ polarization away from the molecules, cf. Fig. 6(a), which decreases the Pauli repulsion between the donating molecular lone pair and the Ni $4s$ electron, and at the same time partially exposes the positive core for better polarization interaction between the molecule and Ni. That it is larger in the $^3\Delta$ states parallels the observations (c) and (d) above, namely, a decreased Ni $3d\sigma$ population for more localized positive charge (versus Ni $4s$) and increased Ni $4s$ population for better polarization (versus Ni $3d$). This population is smallest in the $^1\Sigma^+$ states, again indicating a diminished Ni $4s$ population.

(g) Both the σ donation and the π backward donation are larger in NiCO than in NiN_2. This may be correlated with the fact that the carbon lone pair is more diffuse and

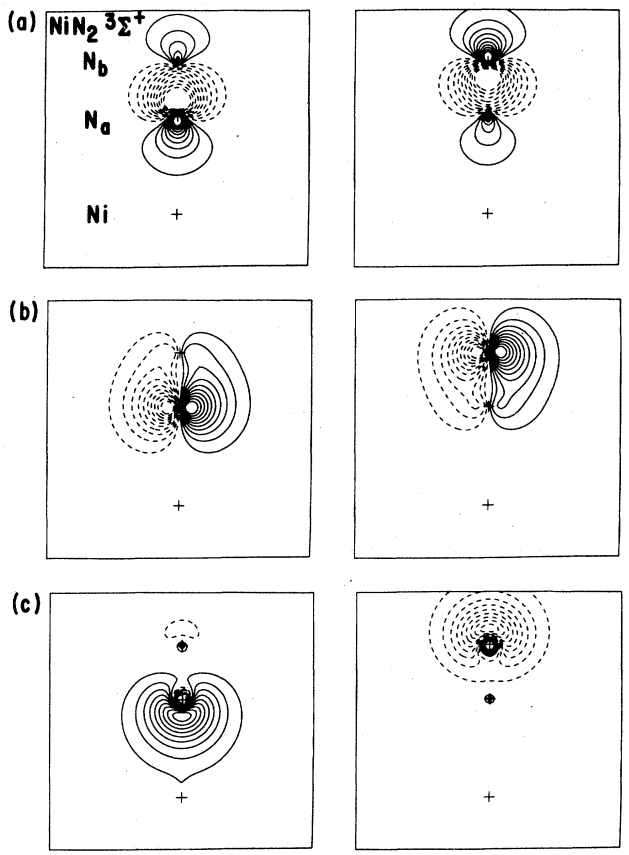

FIG. 5. N_2-derived valence orbital contour plots (in the **y-z** plane) of the GVB-PP wave function for the NiN_2 $^3\Sigma^+$ state at the calculated equilibrium geometry. (a) N_2 GVB σ-bond pair; (b) N_2 GVB π_y-bond pair, there is another equivalent pair (not shown) in the **x-z** plane; (c) the two doubly occupied N_2 lone pairs obtained from combinations of the canonical orbitals.

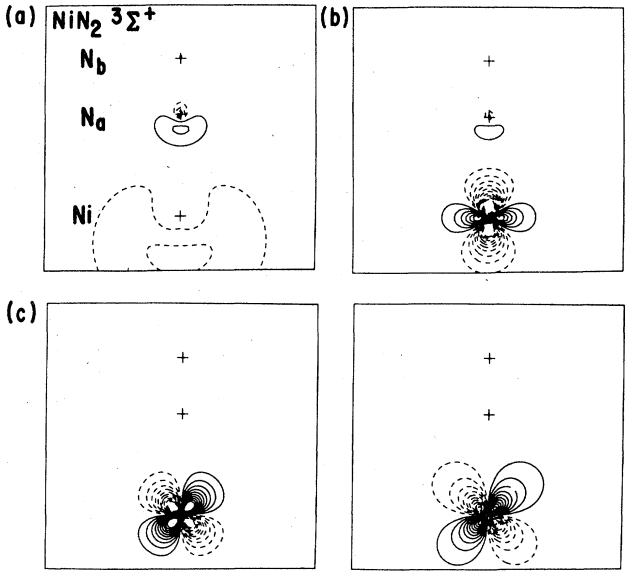

FIG. 6. Ni-derived valence orbital contour plots (in the **y-z** plane) of the GVB-PP wave function for the NiN_2 $^3\Sigma^+$ state at the calculated equilibrium geometry. (a) Ni $4sp\sigma$ (singly occupied); (b) Ni $3d\sigma$ (singly occupied); (c) Ni $3d\pi_y$ pair, there is another equivalent pair (not shown) in the **x-z** plane.

that the virtual 2π orbital of CO is more localized on the carbon.

From the above observations, we may describe the bonding in the $^1\Sigma^+$ states of NiN_2 and NiCO as the usual σ donation (from N_2 and CO) and π backward donation (from Ni); and the bonding in the triplet states as σ donation and π polarization from N_2 or CO towards Ni. The $^1\Sigma^+$ state may be characterized as containing a significant contribution of the Ni $3d^{10}$ configuration in the bonding, whereas the triplet states are characterized by the Ni $3d^9 4s^1$ configurations.

In Table VIII the equilibrium geometries and Ni-molecule bond dissociation energies for the $^1\Sigma^+$, $^3\Sigma^+$, and $^3\Delta$ states of NiN_2 and NiCO are summarized. In both NiN_2 and NiCO, the $^1\Sigma^+$ states were found to be the ground states, with the triplet states being the excited states. The dissociation energies were obtained from dissociation-consistent GVB-D*DCI calculations (see Sec. II), using ^3D Ni plus N_2 or CO as reference. For the $^1\Sigma^+$ states, the dissociation energies were also determined and found to be larger from the GVB-D*QCI calculations (even though they are not dissociation consistent and therefore underestimate the dissociation energy). This observation reinforces the argument that the Ni $3d^{10}$ configuration is indeed important in the bonding in the $^1\Sigma^+$ states, as we recall that the GVB-D*QCI procedure increases the Ni $3d^{10}$ population for the $^1\Sigma^+$ states (cf. Tables VI and VII).

The ordering of the triplet states has been rationalized by Walch and Goddard.[18] Namely, considering the triplet states as arising from Ni $3d^9 4s^1$, the $^3\Sigma^+$ state has a $d\sigma$ hole and thus enjoys the best σ donation from the CO 5σ lone pair, the $^3\Pi$ state has one less $3d_\pi$ electron and thus has the least π backward donation. The two factors (σ donation and π backward donation) would result in the ordering $^3\Sigma^+$, $^3\Delta$ and $^3\Pi$, in increasing energy. On the other hand, in the $^3\Delta$ state, and to a lesser extent, in the $^3\Pi$ state, the Ni ^3F atomic state (d^8s^2), being nearly degenerate with the Ni ^3D state, allows more flexibility. That is, in the d^8s^2 configuration, there are two localized d holes ($d\sigma$ and $d\delta$ or $d\pi$), although there is also more σ repulsion due to double occupation of the Ni $4s$ orbital which, however, may be polarized away from the donating lone pair to partially expose the positive core. The Ni d^8s^2 configuration therefore may play a role in the bonding if the polarization interaction between CO and Ni can offset the additional repulsion between the lone pair and the Ni $4s$ electrons. In any case there is no question that the $^3\Pi$ states lie highest among the triplet states (cf. Tables IV and V).

Walch and Goddard[18] found in NiCO the ordering (in increasing energy) $^3\Delta$, $^3\Sigma^+$, and $^3\Pi$, with consecutive separations of 0.24 and 0.05 eV, respectively. The contribution of the Ni d^8s^2 (^3F) in their calculations, however, might have been overestimated, because the basis set they

TABLE IV. Calculations on the linear NiN_2 molecule. Distances in angstroms, energies and dipole moments in a.u. 1 hartree=27.2116 eV, 1 a.u. dipole moment =2.542 D. The dipole moment is positive if the negative end of the dipole points towards N_2.

			GVB-PP		GVB-D*DCI	
State	R (Ni—N)	R (N—N)	$E+109.0$	μ	$E+109.0$	μ
$^1\Sigma^+$[a]	1.6000	1.1215	−0.534 21	0.832	−0.721 38	0.711
	1.6500	1.1215	−0.537 39	0.727	−0.721 78	0.600
	1.7000	1.1215	−0.538 45	0.625	−0.719 95	0.485
	1.6064	1.1715	−0.526 10	0.878	−0.714 93	0.797
	1.6564	1.0715	−0.534 10	0.655	−0.715 64	0.493
	1.6364	1.1206	−0.536 82	0.754	−0.721 93	0.628
$^1\Sigma^+$[b]	1.6364	1.1206	−0.581 51	−0.659	−0.715 98	−0.346
$^3\Sigma^+$	1.9500	1.1215	−0.605 59	−1.486	−0.714 67	−1.482
	2.0000	1.1215	−0.605 82	−1.444	−0.714 76	−1.441
	2.0500	1.1215	−0.605 53	−1.398	−0.714 35	−1.395
	1.9570	1.1715	−0.596 58	−1.481	−0.705 51	−1.477
	2.0070	1.0715	−0.602 30	−1.437	−0.710 58	−1.433
	1.9873	1.1121	−0.606 26	−1.455	−0.715 17	−1.451
$^3\Delta$	1.9000	1.1215	−0.600 08	−1.553	−0.713 79	−1.554
	1.9500	1.1215	−0.600 87	−1.507	−0.713 99	−1.508
	2.0000	1.1215	−0.601 05	−1.456	−0.713 64	−1.456
	1.9158	1.1715	−0.591 50	−1.536	−0.704 87	−1.536
	1.9658	1.0715	−0.597 33	−1.494	−0.709 66	−1.494
	1.9427	1.1125	−0.601 20	−1.515	−0.714 35	−1.515
$^3\Pi$	1.9500	1.1215	−0.595 26	−1.573	−0.706 47	−1.576
	2.0500	1.1215	−0.597 22	−1.460	−0.707 71	−1.463

[a]Using orbitals obtained by forcing Ni d^{10} configuration; see text (Sec. II).
[b]Using orbitals optimized at the GVB-PP level.

employed was biased in favor of the ^3F Ni state by 0.25 eV relative to the ^3D state. Our calculations, as well as those of Rives and Fenske,[8] result in a smaller $^3\Delta$-$^3\Pi$ splitting in NiCO. But the basis set we used was biased against d^8s^2 (Ref. 13) and against Ni $4p\leftarrow 4s$ excitation (cf. Table I). The calculations for the $^1\Sigma^+$ states were not optimal either as the GVB-PP result is biased against the Ni d^{10} configuration. It is expected that larger CI calculations including virtual orbitals and higher orders of excitation should improve the energies of the $^1\Sigma^+$ states relative to the energies of the triplet states. This is because of the mixing of Ni d^9s^1 and Ni d^{10} character in the wave function as well as the strong π interaction which occurs in the $^1\Sigma^+$ state at short Ni-molecule distances. Both effects require a more highly correlated wave function than obtained here in order to provide a completely consistent treatment. However, this would require a massive computational effort which is not justified in our view at the present. Experimentally, Stevens *et al.* have derived the Ni—CO bond dissociation energy for NiCO to be about 1.3 eV.[19] In that study, the role of the Ni $3d^{10}$ configuration has been convincingly demonstrated and discussed.

It should be pointed out that our calculated dissociation energies for the triplet states of NiCO are close to those found by Walch and Goddard,[18] although ours are somewhat smaller presumably because we did not use virtual orbitals in the CI calculations. On the other hand, Rives and Fenske[8] found the $^3\Delta$ state to be unbound. They attributed the differences to the basis set superposition error. But the effective potential they employed for the Ar core of Ni was biased in favor of d^8s^2 relative to d^9s^1 (see Ref. 13 and Sec. VII of Ref. 18), and we believe their conclusion on this point is incorrect.

With regard to the equilibrium geometries, the $^1\Sigma^+$ state has much shorter Ni—C or Ni—N distance than the triplet states by about 0.3 Å. Again, this observation is consistent with a bonding description in which the $^1\Sigma^+$ states with a significant contribution from the Ni $3d^{10}$ configuration allow shorter Ni-molecule distances (reduced Ni $4s$ repulsion), which in turn facilitates better π backward donation and further shortens the distance. However, because our wave functions cannot describe simultaneously both the Ni d^{10} and the d^9s^1 configurations equally well, we suspect that the calculated Ni—C and Ni—N equilibrium distances for the $^1\Sigma^+$ states are somewhat shorter than reality.

The N—N or C—O intramolecular distance in the Ni-molecule clusters, relative to the free molecules, is elongated somewhat in the $^1\Sigma^+$ states, and is shortened slightly in the triplet states (more so in the $^3\Sigma^+$ states than in the $^3\Delta$ states). These observations may be rationalized as usual in the following: The σ donation, relieving the intramolecular σ repulsion, tends to shorten the bond, while the π backward donation will lengthen the bond.

TABLE V. Calculations on the linear NiCO molecule. Distances in angstroms, energies and dipole moments in a.u. The dipole moment is positive if the negative end of the dipole points towards CO from Ni.

State	R (Ni—C)	R (C—O)	GVB-PP $E+153.0$	GVB-PP μ	GVB-D*DCI $E+153.0$	GVB-D*DCI μ
$^1\Sigma^+$	1.4500	1.1475	−0.351 43	0.805	−0.539 13	0.960
	1.5000	1.1475	−0.362 25	0.597	−0.544 16	0.762
	1.5500	1.1475	−0.370 30	0.308	−0.543 49	0.492
	1.6000	1.1475	−0.376 65	−0.042	−0.538 80	0.180
	1.6500	1.1475	−0.381 81	−0.367	−0.533 33	−0.104
	1.7000	1.1475	−0.385 79	−0.628	−0.528 16	−0.340
	1.4930	1.1975	−0.354 00	0.815	−0.541 70	0.986
	1.5430	1.0975	−0.366 36	0.171	−0.535 47	0.340
	1.5233	1.1637	−0.364 86	0.539	−0.544 96	0.713
$^3\Delta$	1.8500	1.1475	−0.398 16	−1.684	−0.515 53	−1.710
	1.9000	1.1475	−0.399 23	−1.678	−0.515 88	−1.704
	1.9500	1.1475	−0.399 38	−1.661	−0.515 34	−1.688
	1.8695	1.1975	−0.389 03	−1.598	−0.507 52	−1.624
	1.9195	1.0975	−0.398 12	−1.760	−0.512 88	−1.784
	1.8909	1.1353	−0.400 01	−1.700	−0.516 36	−1.725
$^3\Sigma^+$	1.9000	1.1475	−0.400 01	−1.650	−0.511 91	−1.674
	1.9500	1.1475	−0.400 98	−1.640	−0.512 50	−1.665
	2.0000	1.1475	−0.401 10	−1.622	−0.512 28	−1.647
	1.9363	1.1975	−0.390 97	−1.565	−0.503 98	−1.591
	1.9863	1.0975	−0.399 97	−1.710	−0.509 62	−1.732
	1.9613	1.1350	−0.401 97	−1.657	−0.513 02	−1.681
$^3\Pi$	1.9500	1.1475	−0.389 80	−1.743	−0.503 20	−1.772
	2.0000	1.1475	−0.390 92	−1.713	−0.503 84	−1.743

Therefore, the $^1\Sigma^+$ states, with significant π backward donation, result in longer N—N and C—O bonds, while for the triplet states, the σ donation results in shorter bonds.

There are significant differences between NiN_2 and NiCO, however. The Ni-molecule dissociation energy for each state is larger in NiCO than in NiN_2, by $\sim$1, 0.5, and 0.4 eV for the $^1\Sigma^+$, $^3\Delta$, and $^3\Sigma^+$ states, respectively. The $^3\Sigma^+$ state has lower energy than the $^3\Delta$ state in NiN_2, while the opposite is the case in NiCO. The Ni—C distances are all shorter than the Ni—N distances in the corresponding states, by 0.12 Å in the $^1\Sigma^+$ states, 0.06 Å in

TABLE VI. Mulliken population analyses for NiN_2 wave functions. Based on GVB-PP wave functions unless noted otherwise. The populations for the triplet states are about the same at GVB-PP and CI levels, and therefore only the former are listed. N_a is the nitrogen closest to Ni, and N_b is the other nitrogen. Distances in angstroms.

Wave function character \ State	$^1\Sigma^+$	$^1\Sigma^{+a}$	$^1\Sigma^{+b}$	$^1\Sigma^{+c}$	$^3\Sigma^+$	$^3\Delta$	$^3\Sigma^+$	$^3\Delta$
R (Ni—N_a)			1.6364				1.9000	
R (N—N)			1.1206				1.1215	
N_b σ	2.9295	2.9006	2.9054	2.9098	2.9434	2.9474	2.9533	2.9556
N_b π	1.9334	2.0636	2.0345	2.0386	1.9178	1.9098	1.9206	1.9218
N_a σ	2.7648	2.8251	2.8338	2.8042	2.8147	2.8422	2.8857	2.8975
N_a π	2.1182	2.1278	2.1628	2.1582	2.1376	2.1414	2.0948	2.0948
Ni $4s$	1.0485	0.5254	0.5983	0.5812	0.9293	0.9973	0.9212	0.9522
Ni $4p_z$	0.1002	0.0870	0.0833	0.0845	0.2929	0.3246	0.2202	0.2293
Ni $3d\sigma+3d\delta$	5.1574	5.6618	5.6088	5.6207	5.0197	4.8889	5.0200	4.9918
Ni π	3.9486	3.8090	3.8096	3.8031	3.9448	3.9488	3.9846	3.9836

[a]The GVB-PP wave function was forced to be d^{10}-like.
[b]GVB-D*DCI using the set of orbitals as in footnote a.
[c]GVB-D*QCI using the set of orbitals as in footnote a.

TABLE VII. Mulliken population analyses for NiCO wave functions. Based on GVB-PP wave functions unless noted otherwise. The populations for the triplet states are about the same at GVB-PP and CI levels, and therefore only the former are listed. The carbon atom is closer to Ni. Distances in angstroms.

Molecule	CO	NiCO						
State	$^1\Sigma^+$	$^1\Sigma^+$	$^1\Sigma^{+a}$	$^1\Sigma^{+b}$	$^3\Sigma^+$	$^3\Delta$	$^3\Sigma^+$	$^3\Delta$
R (Ni—C)				1.5233			1.9000	
R (C—O)	1.1453			1.1637			1.1475	
Wave function character								
O σ	3.1701	3.1672	3.1616	3.1641	3.1761	3.1748	3.1686	3.1672
O π	2.9374	2.9872	2.9824	2.9854	2.9264	2.9028	2.8910	2.8886
C σ	2.8303	2.2764	2.2532	2.2570	2.3898	2.4489	2.6042	2.6264
C π	1.0626	1.2126	1.2869	1.2882	1.2308	1.2382	1.1454	1.1500
Ni $4s$		0.9300	0.9052	0.8766	0.9179	1.0088	0.9007	0.9360
Ni $4p_z$		0.1131	0.1101	0.1108	0.4759	0.5173	0.3040	0.3183
Ni $3d\sigma+3d\delta$		5.5135	5.5654	5.5916	5.0407	4.8500	5.0228	4.9524
Ni π		3.8002	3.7354	3.7263	3.8428	3.8588	3.9634	3.9616

[a]GVB-D*DCI result.
[b]GVB-D*QCI result.

TABLE VIII. Calculated molecular parameters for NiN_2 and NiCO. Ni-molecule bond dissociation energies (D_e) for $^3\Sigma^+$ and $^3\Delta$ states were obtained from dissociation-consistent (^3D Ni + molecule) GVB-D*DCI calculations, using the lowest energies for each state listed in Tables IV and V. D_e for $^1\Sigma^+$ states were obtained from GVB-D*QCI calculations (relative to DCI on N_2 or CO and QCI on ^3D Ni); the values in parentheses are GVB-D*DCI results. M_1 is the carbon atom in CO or NiCO, and is the nitrogen atom closest to Ni in NiN_2; M_2 is O or N. The equilibrium distances were determined by interpolating the data points listed in Tables IV and V.

System	D_e (eV)	R_e (Ni-M_1) (Å)	R_e (M_1-M_2) (Å)
N_2 $X\,^1\Sigma_g^+$			1.117
NiN_2 $^1\Sigma^+$	0.779 (0.536)	1.634	1.120
NiN_2 $^3\Sigma^+$	0.352	1.986	1.112
NiN_2 $^3\Delta$	0.329	1.944	1.113
CO $X\,^1\Sigma^+$			1.145
NiCO $^1\Sigma^+$	1.77 (1.58)	1.524	1.168
NiCO $^3\Delta$	0.800	1.895	1.136
NiCO $^3\Sigma^+$	0.709	1.960	1.135

TABLE IX. Calculated vibrational properties of NiN_2 and NiCO. Frequencies (ν_1,ν_2) in cm^{-1}, force constants (k_1,k_2) in mdyn/Å. I_1/I_2 is relative intensity. Only stretching modes are considered. Values in parentheses are experimental data, those for matrix-isolated Ni complexes (listed first) are taken from Refs. 2 and 22, and those for chemisorption systems on Ni(110) (listed second) are taken from Ref. 3.

System	ν_1	k_1	ν_2	k_2	I_1/I_2
N_2 $X\,^1\Sigma_g^+$	2374 (2359)	22.4			
NiN_2 $^1\Sigma^+$	2371 (2090, 2190)	22.1	580 (466, 320)	3.94	11.4
NiN_2 $^3\Sigma^+$	2399	23.5	311	1.09	8760
NiN_2 $^3\Delta$	2399	23.4	324	1.19	246
CO $X\,^1\Sigma^+$	2203 (2170)	18.9			
NiCO $^1\Sigma^+$	2012 (1996, 2000)	14.7	607 (, 410)	4.58	28.1
NiCO $^3\Delta$	2238	19.6	395	1.80	0.613
NiCO $^3\Sigma^+$	2243	19.8	381	1.67	0.517

TABLE X. Calculated photoemission properties for NiN_2 and NiCO. Ionization of $1s$ electrons of N_2 and CO in NiN_2 and NiCO. In NiN_2, N_a is the nitrogen closest to the Ni atom, and N_b is the other nitrogen. Ψ^0 is the neutral state, and Ψ^+ is the ion state. [In Ni complexes the screened and the unscreened states are labeled with (s) and (u), respectively.] The ionization energy (IP) is relative to that of the free molecule N_2 or CO. $\langle \Psi^+ \mid \hat{a}\Psi^0 \rangle$ is the overlap, where $\hat{a}$ is the appropriate electron annihilator. I is the intensity relative to the screened peak, and is proportional to the square of the overlap. Experimental values for chemisorbed N_2 and CO on Ni(100) are given in parentheses [taken from Ref. 4, IP's modified by work functions of 5.5 and 6.5 eV for N_2/Ni and CO/Ni, respectively; and referenced to gas-phase values taken from K. Siegbahn *et al.*, *ESCA Applied to Free Molecules* (North-Holland, Amsterdam, 1969)]. See text for details of calculations.

Ψ^0	Ψ^+	IP (eV)	$\langle \Psi^+ \mid \hat{a}\Psi^0 \rangle$	I
$N_2\ {}^1\Sigma_g^+$	$^2\Sigma_u^+$	0.0	0.86	
$NiN_2\ {}^1\Sigma^+$	$N_a\ (s)\ {}^2\Sigma^+$	−4.7 (−4.2)	0.53	1
	$N_a\ (u)\ {}^2\Sigma^+$	−0.6 (+0.9)	0.66	1.5 (1.0)
	$N_b\ (s)\ {}^2\Sigma^+$	−5.0 (−4.2)	0.58	1
	$N_b\ (u)\ {}^2\Sigma^+$	−1.1 (+0.9)	0.62	1.2 (1.0)
$NiN_2\ {}^3\Sigma^+$	$N_a\ (s)\ {}^4\Sigma^+$	+0.8 (−4.2)	0.63	1
	$N_a\ (u)\ {}^4\Sigma^+$	+2.9 (+0.9)	0.46	0.5 (1.0)
CO $^1\Sigma^+$	$C\ {}^2\Sigma^+$	0.0	0.88	
	$O\ {}^2\Sigma^+$	0.0	0.83	
NiCO $^1\Sigma^+$	$C\ (s)\ {}^2\Sigma^+$	−3.9 (−3.8)	0.75	1
	$C\ (u)\ {}^2\Sigma^+$	+0.5 (+1.4)	0.44	0.34 (0.35)
	$O\ (s)\ {}^2\Sigma^+$	−3.9 (−5.1)	0.73	1
	$O\ (u)\ {}^2\Sigma^+$	−1.0 (+0.9)	0.28	0.15 (0.20)

the $^3\Delta$ states, and 0.05 Å in the $^3\Sigma^+$ states. For the $^1\Sigma^+$ states, the increase in the C—O distance in NiCO, 0.019 Å, is much larger than the corresponding increase in the N—N distance of NiN_2, 0.004 Å. Once again, all these differences reflect the fact that in the triplet states the main interaction is σ donation and π polarization from the molecule towards Ni. This is more favorable in NiCO because the carbon lone pair is more diffuse and the molecular polarizability of CO ($\alpha_{\parallel} = 15.55a_0^3$, $\alpha_{\perp} = 11.86a_0^3$) (Ref. 20) is larger than that of N_2 ($\alpha_{\parallel} = 14.82a_0^3$, $\alpha_{\perp} = 10.20a_0^3$).[21] In the $^1\Sigma^+$ states the bonding includes the important π backward donation which is also more favorable in NiCO because the C—O π bonds are polarized towards the oxygen. In addition, CO provides better σ donation.

B. Vibrational and photoemission properties

Experimentally, the most direct observations regarding NiCO and NiN_2 have been the vibrational spectra, most of them taken from matrix-isolated samples.[1,17,19,22] The decreases in the N—N and C—O stretching frequencies upon complexing with Ni atoms reveal the significance of Ni-molecule interactions. The vibrational frequencies of the free N_2 and CO molecules are 2359 and 2170 cm^{-1}, respectively,[7] whereas in NiN_2 and in NiCO isolated in matrices, the corresponding frequencies are 2090 and 1996 cm^{-1}, respectively.[1,22] This downward shift in vibrational frequencies should be reproduced if the theoretical potential surfaces and the assumption about the electronic ground states are realistic. We have calculated the stretching frequencies, as well as their relative intensities,[23] using the data points given in Tables IV and V (GVB-D*DCI results), and assuming the simple harmonic valence force-field approximation.[24] The results are listed in Table IX. In comparison with the calculated free-molecule values (obtained with the same harmonic-oscillator approximation, cf. Tables II and III), the N—N or C—O stretching force constant and associated frequency do not decrease in the $^3\Delta$ and $^3\Pi$ states of NiN_2 or NiCO. In fact, they increase very slightly, consistent with the fact that the N—N and C—O bond lengths are shortened slightly in these triplet states. The upward shift of the vibrational frequencies in these triplet states is inconsistent with experiment in regard to the ground-state behavior of the NiN_2 and NiCO species.[1,22] The $^1\Sigma^+$ state of NiCO gives the correct downward shifts for both the frequency and force constant. It should be pointed out, however, that here the fitting of the potential surface is accurate only to the order of the Ni—CO stretching frequency, due to a lack of smoothness of the calculated potential surface (cf. Table V). This lack of smoothness is almost surely an artifact of our calculations. Namely, in the $^1\Sigma^+$ state, the dominant configuration of the Ni atom changes from d^9s^1 (singlet) at large Ni—CO distances to a mixture of d^9s^1- and d^{10}-like character near the equilibrium geometry. However, our calculations are biased in favor of the d^9s^1 configuration and hence cannot describe properly the potential surface near the d^9s^1-d^{10}-like transition region. Nonetheless, the calculated decrease of the C—O stretching frequency (which is predominantly determined by the C—O bond strength) is judged to be of physical significance. With regard to the vibrational spectrum

for the $^1\Sigma^+$ state of NiN_2, the problem associated with the calculated potential surface is probably even more severe, as we may recall that we have forced the wave functions there to be d^{10}-like—a procedure which tends to overestimate the Ni—N_2 stretching force constant and consequently results in a higher N—N stretching frequency. Nonetheless, the calculated N—N force constant decreases, in agreement with the experiment. We note in passing that the magnitudes of the downward shifts of the N—N and C—O stretching frequencies do not depend solely on the degree of weakening of the N—N and C—O bonds (or the degree of π backward donation), because the frequencies are also influenced by the Ni-molecule bond strengths. Thus, our calculations suggest that the smaller shift of the C—O stretching frequency in NiCO as compared to the N—N shift in NiN_2 may be attributed to the stronger Ni—CO bond, rather than to a stronger Ni—N_2 π backward donation.

The significant differences in electronic structure between the $^1\Sigma^+$ and the triplet states for NiN_2 or NiCO is also expected to be reflected in their photoemission spectra (PES). There is no experimental PES on isolated NiN_2 or NiCO, but for chemisorbed N_2 on the Ni(100) surface, the experimental PES shows two strong peaks separated by 5 eV with about equal intensity in the nitrogen core region.[4,25]

In Table X some results are listed for the photoemission of N_2 and CO core electrons in NiN_2 and NiCO. The focus here is to evaluate the role of Ni $3d$ electrons in the ion states. So we have obtained two types of GVB-PP wave functions, one is characterized by the Ni $3d\pi$ charge-transfer screening (screened), and the other one without this screening (unscreened). It should be pointed out that these GVB-PP wave functions are not orthogonal, so the relative ionization energies between screened and unscreened states listed in Table X are underestimated in this regard, except for the NiN_2 $^3\Sigma^+$ state ionizations which were obtained from interaction-matrix diagonalized wave functions.[26] On the other hand, the unscreened GVP-PP wave functions for ionizations from $^1\Sigma^+$ states are expected to have more correlation error as they have Ni d^{10} configurations, which would overestimate the ionization separation when the screened (Ni^+ d^9-like) state has lower energy. These two sources of error tend to cancel each other for ionizations from $^1\Sigma^+$ states, the results listed in Table X are therefore probably correct to 1 eV (judged from experience). Another point to note is that the GVB-PP wave functions for the screened states are obtained as mixtures of Σ^+ and Δ states. Restoration of symmetry[27] lowered the energy by 0.6 eV in the case of the NiN_2^+ $^2\Sigma^+$ state. The procedure was not applied for the NiCO case, but the same lowering of 0.6 eV was included for the values given in Table X. The calculated relative photoemission intensity was based on the overlap approximation.[28] For the ionizations from the $^1\Sigma^+$ states, the wave functions used to calculate overlaps were symmetry projected for the screened ion states and Schmidt orthogonalized (against the screened state) for the unscreened ion states.

The results shown in Table X indicate that the $^1\Sigma^+$ states of NiN_2 and NiCO lead to reasonable agreement with the experimental data, in terms of both energy separations and relative intensities between the screened and unscreened states, for the corresponding chemisorbed systems. Whereas the $^3\Sigma^+$ state of NiN_2 cannot account for the lowering of the ionization energy ($+0.8$ eV calculated versus -4.2 eV experiment) due to the charge-transfer screening mechanism. As mentioned earlier, the ionization energy of a Ni $3d$ electron (which is involved in the energetics of the screening process and has been used as an indicator for Ni π backward donation in the neutral), 5.8 eV for $d^{10}\rightarrow d^9$, and 8.7 eV for $d^9s^1(^3D)\rightarrow d^8s^1(^4F)$, explains why the $^1\Sigma^+$ state with a significant admixture of the Ni d^{10} configuration leads to much more favorable Ni $d\pi$ screening.

For the $^1\Sigma^+$ state of NiN_2, the calculated core-ionization energies for the two nitrogens are different by ≥ 0.3 eV for both the screened and unscreened relaxation processes; with the ionization energies from the nitrogen closer to the Ni atom being larger. Egelhoff[29] has interpreted his experiments as suggesting an inequivalence of the two nitrogen core-ionization energies (screened) for the N_2/Ni(100) system, and has likened this inequivalence, employing the equivalent-core approximation, to the difference in the chemisorption energy between NO/Ni (oxygen end of NO bonded to Ni) and ON/Ni (nitrogen end bonded). However, the 1.1-eV inequivalence he found is much larger than the 0.3 eV from our present calculations. The origin of this discrepancy and a detailed investigation of the inequivalent N $1s$ hole states are discussed elsewhere.[30]

IV. NiN_2 AND NiCO AS MODELS FOR CHEMISORPTION

We have found the ground state for both NiN_2 and NiCO to be a $^1\Sigma^+$ state characterized by a significant Ni $3d^{10}$ component in the wave function. In contrast, the triplet states are predominantly derived from the Ni $3d^94s^1$ configuration. The differences in electronic structure between these two types of states are reflected in the following results: the $^1\Sigma^+$ states have shorter Ni-molecule distances, decreased molecular stretching frequencies, and dipole moments with the negative ends pointing towards the N_2 and CO molecules. These properties of the $^1\Sigma^+$ states, as well as their calculated PES, exhibit the same behavior as the experimental data for N_2 and CO chemisorption on Ni surfaces, thus strongly suggesting that the bonding in these chemisorption systems is predominantly local in nature and that the Ni $3d^{10}$ configuration is important for chemisorbed CO and N_2. Indeed, this hypothesis may have support in a recent experimental study.[31]

The calculated properties of the $^1\Sigma^+$ states can be easily understood in terms of the Ni $3d^{10}$ component in the wave function which results in π back bonding between Ni and CO or Ni and N_2 being facilitated. This naturally yields the downward shift of the CO or N_2 stretching frequency. Furthermore, the π backward donation also results in a dipole moment with its negative end pointing towards CO or N_2, i.e., there is an electronic polarization towards CO or N_2 chemisorbed on Ni surfaces. Experimentally, such polarization has been inferred from the in-

crease in the work function ($\Delta\phi > 0$) (Ref. 32) upon chemisorption of CO or N_2 on Ni surfaces. In fact, the correlation between the vibrational frequency shift and $\Delta\phi$ has been discussed and attributed to the π back bonding by Nieuwenhuys.[33] In cases in which π backward donation is not significant, such as in CO adsorbed on Cu surfaces,[34] or not possible, such as in Xe physisorption,[35] the only major interaction expected is σ donation and/or π polarization from the adsorbate. This results in a dipole moment with its negative end pointing toward the bulk metal, similar to the situation for the triplet states we have seen in this paper. Therefore, in these cases $\Delta\phi < 0$ is expected, which is consistent with experiment.

The relative peak intensities in the core photoemission data also suggest that the bonding of N_2 and CO on Ni surfaces involves the Ni d^{10} configuration. The high intensities for the metal charge-transfer screened peaks can be traced to the significant π backward donation in the neutral states. The π backward donation, however, occurs most significantly only in the Ni d^{10} configuration. Although the metal s-p band can also be involved in bonding by symmetry, it alone cannot account for the PES intensities, as demonstrated in detail elsewhere.[3] That the π backward donation from the metal s-p band is not significant may arise from the following two effects. Firstly, the Ni $3d^9 4s^1$ configuration restricts the Ni-molecule separations to larger distances, which would decrease π backward donation. Secondly, the π backward donation is not independent of the σ interaction, i.e., the large Pauli repulsion between the donating molecular lone pair and the Ni $4s$ electron in the Ni $3d^9 4s^1$ configuration limits the extent of σ donation, which in turn would limit the extent of π backward donation.

The Ni-molecule distance is another parameter which can be used to discern the electronic configuration of the surface Ni atoms bonding with N_2 or CO. There have been a few low-energy electron diffraction (LEED) determinations for CO chemisorbed on the Ni(100) surfaces,[36] suggesting a Ni—C distance between 1.72 to 1.80 Å. Assuming the Ni $3d^9 4s^1$ configuration, Allison and Goddard[37] found the Ni—C distance to be 1.94 Å from their $Ni_{14}CO$ cluster studies. This is close to the distances we have found for the $^3\Delta$ (1.89 Å) and $^3\Sigma^+$ (1.96 Å) states of NiCO, but is rather longer than the LEED results suggest. On the other hand, the LEED results do not support the 1.52 Å distance we find for the Ni d^{10} configuration (the $^1\Sigma^+$ state) either. However, it is expected that improving the quality of both the basis set and wave function for the $^1\Sigma^+$ state should lengthen the calculated Ni—C equilibrium distance somewhat as discussed above.

V. SUMMARY

We have found the ground states for both NiN_2 and NiCO to be $^1\Sigma^+$ states with significant Ni $3d^{10}$ character in the wave function. This had led to calculated properties consistent with experimental observations even in chemisorption situations.

Namely, we have considered the dipole moment, the work-function change, the vibration and photoemission spectroscopies (in terms of both energy and intensity), as well as the bond energies. It is interesting that all these properties for the $^1\Sigma^+$ state for both NiN_2 and NiCO are consistent with the experimental data for the corresponding chemisorption systems.

The present study strongly suggests that local changes in electronic configuration induced by chemisorption may be important in understanding the nature of transition-metal-molecule surface interactions. Local atomic configurational changes may also be a key to the understanding of transition-metal reactivity and catalysis. This is a phenomenon which has received little or no attention previously in the surface literature.

The importance of calculating the widest possible variety of physical properties of the chemisorption system in order to compare with available experimental data should be apparent from this study. Simple models based on approximate wave functions may be misleading if we evaluate only a few properties and obtain agreement with experiment. The essential physics of such a model may be quite different from that necessary to consistently describe a wide variety of properties. It is rather critical for complicated systems, such as chemisorption on transition metals, that we provide the most stringent tests of our models which we can devise. Only in this way can we hope to approach some understanding of the true nature of transition-metal-molecule interactions.

ACKNOWLEDGMENT

This work was supported in part by the U. S. Office of Naval Research.

[1] W. Klotzbucher and G. A. Ozin, J. Am. Chem. Soc. **97**, 2672 (1975).

[2] K. Horn, J. DiNardo, W. Eberhardt, H.-J. Freund, and E. W. Plummer, Surf. Sci. **118**, 465 (1982).

[3] C. M. Kao and R. P. Messmer (unpublished).

[4] P. S. Bagus, C. R. Brundle, K. Hermann, and D. Menzel, J. Electron Spectrosc. Related Phenom. **20**, 253 (1980); P. S. Bagus, K. Hermann, and M. Seel, J. Vac. Sci. Technol. **18**, 435 (1981); K. Hermann, P. S. Bagus, C. R. Brundle, and D. Menzel, Phys. Rev. B **24**, 7025 (1981); C. R. Brundle, P. S. Bagus, D. Menzel, and K. Hermann, *ibid.* **24**, 7041 (1981).

[5] D. A. King, Surf. Sci. **9**, 375 (1968); M. Grunze, R. K. Driscoll, G. N. Burland, J. C. L. Gornish, and J. Pritchard, Surf. Sci. **89**, 381 (1979).

[6] J. J. Turner, M. B. Simpson, M. Poliakoff, and W. B. Maier II, J. Am. Chem. Soc. **105**, 3898 (1983).

[7] K. P. Huber and G. Herzberg, *Molecular Spectra and Molecular Structure,* Vol. IV of *Constants of Diatomic Molecules* (Van Nostrand, Princeton, 1979).

[8] A. B. Rives and R. F. Fenske, J. Chem. Phys. **75**, 1293 (1981).

[9] B. I. Dunlap, H. L. Yu, and P. R. Antoniewicz, Phys. Rev. A **25**, 7 (1982).

[10] R. A. Bair, W. A. Goddard III, A. F. Voter, A. K. Rappe, L. G. Yaffe, F. W. Bobrowicz, W. R. Wadt, P. J. Hay, and W. J. Hunt, GVB2P5 program code (unpublished); see R. A. Bair, Ph.D. thesis, California Institute of Technology, 1980; F. W. Bobrowicz and W. A. Goddard III, in *Methods of Electronic Structure Theory,* edited by H. F. Schaefer III (Plenum, New

York, 1977), Vol. 3, pp. 79—127; W. J. Hunt, P. J. Hay, and W. A. Goddard III, J. Chem. Phys. **57**, 738 (1972).

[11]T. H. Dunning, Jr. and P. J. Hay, in *Methods of Electronic Structure Theory,* edited by H. F. Schaefer III (Plenum, New York, 1977), Vol. 3, pp. 1—27.

[12]T. H. Upton and W. A. Goddard III, in *Chemistry and Physics of Solid Surfaces,* edited by T. Vanselow and W. England (CRC, Boca Raton, 1982), Vol. 3, pp. 127—162.

[13]The double-zeta basis set for the $3d$ orbital was contracted from five primitives optimized for the d^{10} configuration [taken from the article by A. K. Rappe, T. A. Smedley, and W. A. Goddard III, J. Phys. Chem. **85**, 2607 (1982)]. We also did several calculations using a triple-zeta basis set contracted from six primitives (taken from the same reference above) and observed no qualitative differences. The double-zeta $4s$ and $4p$ basis sets were taken from Ref. 12.

[14]The number of configurations for the $^3\Sigma^+$ state was less than that for the $^1\Sigma^+$ state because in the former we did not allow excitations from Ni $4s$ and $3d_{z^2}$ into N_2 or CO σ orbitals for a technical reason. This restriction was not important, and in fact could have been imposed on other states as well, for we did one calculation adding such excitations for the $^3\Sigma^+$ state (some triple excitations on Ni were included) at a short Ni—N distance of 1.64 Å and the energy improved by less than 0.0002 hartree.

[15]C. E. Moore, in *Atomic Energy Levels,* Natl. Bur. Stand. (U.S.) Spec. Pub. No. 467 (U.S. G.P.O., Washington, D.C., 1952), Vol. II.

[16]R. S. Mulliken, J. Chem. Phys. **23**, 1833 (1955).

[17]E. P. Kundig, D. McIntosh, M. Moskovits, and G. A. Ozin, J. Am. Chem. Soc. **95**, 7234 (1973).

[18]S. P. Walch and W. A. Goddard III, J. Am. Chem. Soc. **98**, 7908 (1976).

[19]A. E. Stevens, C. S. Feigerle, and W. C. Lineberger, J. Am. Chem. Soc. **104**, 5026 (1982).

[20]M. P. Bogaard, A. D. Buckingham, R. K. Pierens, and A. H. White, J. Chem. Soc. Faraday Trans. I **74**, 3008 (1978).

[21]G. D. Zeiss and W. J. Meath, Mol. Phys. **33**, 1155 (1977); R. H. Orcutt and R. H. Cole, J. Chem. Phys. **46**, 697 (1967); N. J. Bridge and A. D. Buckingham, Proc. R. Soc. London Ser. A **295**, 334 (1966); A. C. Newell and R. C. Baird, J. Appl. Phys. **36**, 3751 (1965).

[22]R. L. DeKock, Inorg. Chem. **10**, 1205 (1971).

[23]The intensity is assumed to be proportional to $\nu\langle\psi_1|\mu|\psi_0\rangle^2$, where ψ_1 and ψ_0 are the first excited- and ground-state harmonic-oscillator wave functions, respectively, and μ is the electric dipole operator, all in normal coordinates. Anharmonicity was disregarded in the calculations.

[24]G. Herzberg, *Molecular Spectra and Molecular Structure,* Vol. II of *Infrared and Raman Spectra of Polyatomic Molecules* (Van Nostrand, Princeton, 1945), p. 173.

[25]C. R. Brundle and A. F. Carley, Discuss. Faraday Soc. **60**, 51 (1975).

[26]The screened (broken symmetry) and unscreened GVB-PP wave functions for NiN_2 $^3\Sigma^+$ state ionizations were nearly degenerate ($\Delta E = -0.3$ eV), and therefore Schmidt orthogonalization was not employed. Instead, eigenfunctions were obtained by diagonalizing the interaction matrix. For the method of calculation, see Ref. 27.

[27]A. F. Voter and W. A. Goddard III, Chem. Phys. **57**, 253 (1981).

[28]R. L. Martin and D. A. Shirley, in *Electron Spectroscopy: Theory, Techniques and Applications,* edited by C. R. Brundle and A. D. Baker (Academic, New York, 1977), Vol. I, p. 75.

[29]W. F. Egelhoff, Jr., Phys. Rev. B **29**, 3681 (1984).

[30]H.-J. Freund, R. P. Messmer, C. M. Kao, and E. W. Plummer, following paper [Phys. Rev. B **31**, 4848 (1985)].

[31]W. F. Egelhoff, Jr., J. Vac. Sci. Technol. A **2**, 932 (1984); P. W. Selwood, *Chemisorption and Magnetization* (Academic, New York, 1975), pp. 100—107.

[32]J. Campuzano, R. Dus, and R. G. Greenler, Surf. Sci. **102**, 172 (1981).

[33]B. E. Nieuwenhuys, Surf. Sci. **105**. 505 (1981).

[34]S. A. Lindgren, J. Paul, and L. Wallden, Surf. Sci. **117**, 426 (1982).

[35]K. Christmann and J. E. Demuth, Surf. Sci. **120**, 291 (1982).

[36]M. Passler, A. Ignatiev, F. Jona, D. W. Jepsen, and P. M. Marcus, Phys. Rev. Lett. **43**, 360 (1979); S. Andersson and J. B. Pendry, Surf. Sci. **71**, 75 (1978); Phys. Rev. Lett. **43**, 363 (1979).

[37]J. N. Allison and W. A. Goddard III, Surf. Sci. **115**, 553 (1982).